ISSN 0016-7037
Volume 75, Number 17
September 1, 2011

Geochimica et Cosmochimica Acta

JOURNAL OF THE GEOCHEMICAL SOCIETY
AND THE METEORITICAL SOCIETY

Volume 75, Number 17 September 1, 2011

Articles

Continued on outside back cover

Available online at www.sciencedirect.com
ScienceDirect
Geochimica et Cosmochimica Acta 75 (2011) 4987–4997
Geochimica et Cosmochimica Acta
www.elsevier.com/locate/gca

Stable calcium isotopic compositions of Hawaiian shield lavas: Evidence for recycling of ancient marine carbonates into the mantle

Shichun Huang *, Juraj Farkaš [1], Stein B. Jacobsen

Department of Earth and Planetary Sciences, Harvard University, 20 Oxford St., Cambridge, MA 02138, United States

Received 15 February 2011; accepted in revised form 8 June 2011; available online 16 June 2011

Abstract

We report high-precision $^{44}Ca/^{40}Ca$ measurements ($2\sigma_m < 0.06‰$) of Hawaiian shield stage tholeiites. Our data reveal ~0.3‰ variation in their $^{44}Ca/^{40}Ca$, which comprises ~20% of the $^{44}Ca/^{40}Ca$ variation observed in global carbonates. The $^{44}Ca/^{40}Ca$ variation is correlated with Sr/Nb and $^{87}Sr/^{86}Sr$, and this pattern is best explained by adding up to 4% ancient carbonate into the Hawaiian plume. Mass-balance calculations show that up to 40% of the Ca budget and 65% of the Sr budget in some Hawaiian (Makapuu-stage Koolau) lavas are derived from recycled carbonates. Our finding demonstrates, for the first time with the application of Ca isotopes, that ancient recycled carbonates are important components of mantle plumes which feed some of the largest terrestrial volcanoes. Thus, recycling of carbonates into the mantle is an essential part of the global Ca and C cycles.

1. INTRODUCTION

Over geological time, marine carbonates represent one of the most important sinks of atmospheric CO_2. The global Ca and C cycles are intimately linked and their mutual interactions modulate the atmospheric CO_2 level, which in turn controls the climate (DePaolo, 2004). Recycling of marine carbonates into the mantle through subduction zones (e.g., Plank and Langmuir, 1993; Dasgupta et al., 2004; DePaolo, 2004) is an important part of the global Ca and C cycles. This process significantly modifies the volume of surface CO_2 sinks, and potentially introduces Ca and C isotopic variations within the mantle (DePaolo, 2004), because marine carbonates typically have lighter Ca (De La Rocha and Depaolo, 2000; DePaolo, 2004; Fantle and Depaolo, 2005; Heuser et al., 2005; Kasemann et al., 2005; Farkaš et al., 2007a,b; Griffith et al., 2008) and heavier C (Shields and Veizer, 2002) isotopic compositions compared to typical mantle values (DePaolo, 2004; Amini et al., 2009; Huang et al., 2010; Simon and Depaolo, 2010). Although it has been suggested that recycling of marine carbonates into the mantle can introduce lighter Ca isotopic compositions within the mantle (DePaolo, 2004), so far there has been no available Ca isotopic data on mantle-derived rocks supporting this hypothesis. In this study, we test this hypothesis using Hawaiian lavas.

The Hawaiian plume, which feeds the Hawaiian volcanoes, is thought to originate from the lower mantle (Brandon et al., 1999; Humayun et al., 2004; Montelli et al., 2004). It has been suggested based on geochemical studies of Hawaiian lavas that recycled ancient marine sediments are important in the petrogenesis of Hawaiian lavas (Frey et al., 1994; Lassiter and Hauri, 1998; Blichert-Toft et al., 1999). Based on Rb/Sr–$^{87}Sr/^{86}Sr$ correlations within Hawaiian lavas, it is further argued that this recycled ancient marine sedimentary component in Hawaiian lavas is carbonate-rich (Huang and Frey, 2005; Huang et al., 2009). Specifically, within Hawaiian lavas, Makapuu-stage

* Corresponding author. Tel.: +1 617 496 7393.
E-mail addresses: huang17@fas.harvard.edu (S. Huang), juraj.farkas@geology.cz (J. Farkaš).
[1] Present address: Department of Geochemistry, Czech Geological Survey, Geologicka 6, 152 00 Prague 5, Czech Republic.

0016-7037/$ - see front matter © 2011 Elsevier Ltd. All rights reserved.
doi:10.1016/j.gca.2011.06.010

Koolau lavas have the highest $^{87}Sr/^{86}Sr$ (Roden et al., 1994; Lassiter and Hauri, 1998) and the lowest Rb/Sr (Roden et al., 1994; Huang et al., 2009). Apparently, the high $^{87}Sr/^{86}Sr$ in Makapuu-stage Koolau lavas cannot be explained as the result of in situ radiogenic ingrowth of ^{87}Sr from ^{87}Rb. Thus, it has been suggested that the high-$^{87}Sr/^{86}Sr$, low-Rb/Sr endmember in Hawaiian lavas, which is best manifested in Makapuu-stage Koolau lavas, reflects a role of recycled ancient carbonates (Huang et al., 2009). This is because marine carbonates inherit $^{87}Sr/^{86}Sr$ from the coeval seawater from which they crystallized, and since 2.5 Ga the seawater $^{87}Sr/^{86}Sr$ was more radiogenic than that of the coeval mantle (Shields and Veizer, 2002). The importance of a recycled carbonate component in the Hawaiian plume is also consistent with the oxygen isotopic data in olivines from Hawaiian lavas. In detail, olivines from Makapuu-stage Koolau lavas have $\delta^{18}O$ higher than typical mantle values (Eiler et al., 1996; Lassiter and Hauri, 1998), implying a role of recycled materials, which either experienced low temperature alteration or precipitated at low temperature such as marine carbonates, in the source of Makapuu-stage Koolau lavas. As discussed above, a recycled ancient carbonate-rich sedimentary component within the Hawaiian plume can introduce Ca isotopic variations within Hawaiian lavas (DePaolo, 2004). If this is the case, then the Ca isotopic compositions of Hawaiian lavas should correlate with geochemical parameters that are controlled by the recycled ancient carbonates, such as Sr/Nb and $^{87}Sr/^{86}Sr$ (Huang and Frey, 2005; Huang et al., 2009).

In order to test this idea, we analyzed the stable Ca isotopic compositions of 11 tholeiites from four Hawaiian volcanoes (Koolau, Mahukona, Mauna Kea and Kilauea), using a ^{43}Ca–^{48}Ca double spike technique (Russell et al., 1978; Heuser et al., 2002; Huang et al., 2010). Specifically, three ratios are reported:

$$\delta^{44/40}Ca^{sample}_{SRM915a} = \left[\frac{\left(\frac{^{44}Ca}{^{40}Ca}\right)_{sample}}{\left(\frac{^{44}Ca}{^{40}Ca}\right)_{SRM915a}} - 1\right] \cdot 10^3 \quad (1)$$

$$\delta^{42/40}Ca^{sample}_{SRM915a} = \left[\frac{\left(\frac{^{42}Ca}{^{40}Ca}\right)_{sample}}{\left(\frac{^{42}Ca}{^{40}Ca}\right)_{SRM915a}} - 1\right] \cdot 10^3 \quad (2)$$

$$\delta^{44/42}Ca^{sample}_{SRM915a} = \left[\frac{\left(\frac{^{44}Ca}{^{42}Ca}\right)_{sample}}{\left(\frac{^{44}Ca}{^{42}Ca}\right)_{SRM915a}} - 1\right] \cdot 10^3 \quad (3)$$

2. ANALYTICAL DETAILS

About 10 mg rock powders were dissolved using 1:1 mixture of HF and HNO_3 acids in Telfon beakers at 120 °C for 2 weeks. The sample solution was dried down, and then it was dried down three times with concentrated HNO_3 and once with 6 N HCl in order to break insoluble CaF_2. Finally, the sample was dissolved in 2.5 N HCl. No residue was observed in any of our samples. This HF–HNO_3 digestion procedure was proven not to introduce any Ca isotopic fractionation (Huang et al., 2010).

An aliquot of sample solution containing 20 μg Ca was mixed with an appropriate amount of the ^{43}Ca–^{48}Ca double spike solution, so that the $^{40}Ca/^{48}Ca$ (sample to spike ratio) of the spiked sample is between 30 and 80. This range of sample to spike ratios has been proven to be optimal for determining the Ca isotopic compositions (Huang et al., 2010). The spiked sample solution was then dried down, and dissolved in 10 μL 2.5 N HCl. Then it was loaded onto a Teflon micro-column filled with 250 μL cation exchange resin BioRad AG50W-X12, and Ca was purified from the sample solution following the column chemistry procedure documented in the Appendix of Huang et al. (2010). The column chemistry was carefully calibrated to ensure 100% Ca yield. Each sample was passed through the column twice in order to ensure that the final Ca cut is free of matrix elements, especially K and Ti.

About 5 μg purified Ca was loaded as calcium nitrate onto a side filament of a Re triple filament assembly. The Ca isotopic compositions were determined at Harvard University with a GV IsoprobeT TIMS using a two-sequence method. The first sequence collects masses ^{40}Ca, ^{41}K, ^{42}Ca, ^{43}Ca and ^{44}Ca, and the second ^{44}Ca and ^{48}Ca. Before and after data collection, the mass range from 39 to 49 was carefully scanned, and no ^{47}Ti, ^{49}Ti or doubly charged ^{87}Sr peaks have been observed in any of our analyzed samples. Before data collection, baselines and each Ca peak were carefully checked to ensure that there were no reflected ions or electrons perturbing isotopic measurements. Baselines were measured at mass 46.5 for 30 s before each block. Each analysis consisted of 20 blocks, 10 cycles each, using a 6 s integration time for each sequence, followed by a 1 s waiting time. The ^{40}Ca beam intensity was kept at about 8 V during our typical isotopic measurements. A possible isobaric interference of ^{40}K on ^{40}Ca was corrected online using $^{40}K/^{41}K = 1.7384 \times 10^{-3}$. The ^{41}K beam intensity was less than 0.05 V in all our analyzed samples, and less than 0.01 V in most samples. Consequently, ^{40}K correction on ^{40}Ca was less than 10 ppm, much smaller than our analytical errors (Table S1). Typically, the in-run instrumental isotopic fractionation of $^{44}Ca/^{40}Ca$ was less than 0.5‰. The total procedural Ca blank was less than 25 ng.

The mass dependent Ca isotopic ratios, expressed as $\delta^{4i/4j}Ca$ relative to NIST SRM915a standard (Eqs. (1)–(3)), were determined by a ^{43}Ca–^{48}Ca double spike technique using an offline data reduction procedure with an exponential law adopted from Heuser et al. (2002). Details of the approach are approach is given in the Appendix of Huang et al. (2010). Each sample was analyzed multiple times, and the analytical uncertainty (two standard error) was estimated based on multiple measurements (Table S1). The long-term (since 2007) external reproducibility of $\delta^{44/40}Ca_{SRM915a}$ in NIST SRM915a and IAPSO seawater was summarized in Fig. 1.

Two ^{43}Ca–^{48}Ca double spike solutions were used in this study. They were both made from isotopically enriched carbonates, Ca43-NX and Ca48-RT, available from Oak Ridge National Laboratory, following the procedure described in the Appendix of Huang et al. (2010). These two ^{43}Ca–^{48}Ca double spike solutions have very similar isotopic

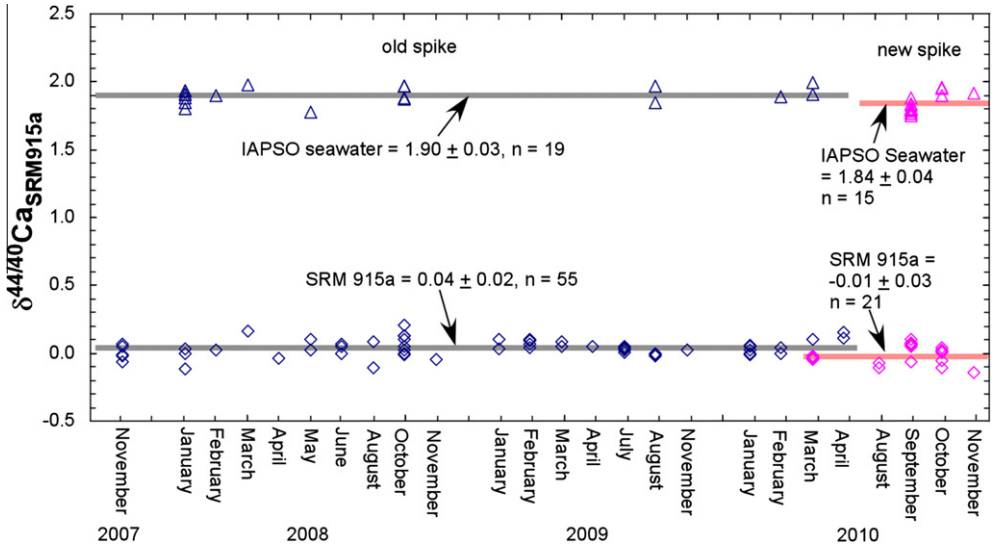

Fig. 1. Long-term (over 3 years) $\delta^{44/40}Ca_{SRM915a}$ measurements of NIST SRM915a and IAPSO seawater obtained with the IsoProbe-T at Harvard University. Two ^{43}Ca–^{48}Ca double spike solutions (Table 1) have been used during the course of our analysis. $\delta^{44/40}Ca_{SRM915a}$ of two standard samples measured using these two spikes agree within analytical uncertainty (see text for a detailed discussion). There is no long-term $\delta^{44/40}Ca_{SRM915a}$ drift in our measured standard samples.

Table 1
Isotopic compositions of two ^{43}Ca–^{48}Ca double spike solutions.

	Old	New
$^{40}Ca/^{48}Ca$	0.11710	0.11424
$^{42}Ca/^{48}Ca$	0.0071862	0.0071825
$^{43}Ca/^{48}Ca$	0.72206	0.72161
$^{44}Ca/^{48}Ca$	0.044317	0.044237

compositions, and their isotopic compositions are in Table 1.

There are no measureable differences between Ca isotopic compositions determined by these two ^{43}Ca–^{48}Ca double spike solutions. NIST SRM915a yields $\delta^{44/40}Ca_{SRM915a} = 0.04 \pm 0.02$ ($n = 55$, $2\sigma_m$) using the old double spike solution, and $\delta^{44/40}Ca_{SRM915a} = -0.01 \pm 0.03$ ($n = 21$, $2\sigma_m$) using the new double spike solution; they agree within analytical errors. Similarly, IAPSO seawater yields $\delta^{44/40}Ca_{SRM915a} = 1.90 \pm 0.03$ ($n = 19$, $2\sigma_m$) using the old double spike solution, and $\delta^{44/40}Ca_{SRM915a} = 1.84 \pm 0.04$ ($n = 15$, $2\sigma_m$) using the new double spike solution; they also agree within analytical errors, and these values are consistent with previous reported values (e.g., Hippler et al., 2003; Amini et al., 2009). This is also true for our analyzed Hawaiian tholeiites. For example, sample BHVO-1 was analyzed using both double spike solutions (Table S1). It yields $\delta^{44/40}Ca_{SRM915a} = 1.00 \pm 0.09$ ($n = 4$) using the old double spike solution, and $\delta^{44/40}Ca_{SRM915a} = 0.92 \pm 0.03$ ($n = 5$) using the new double spike solution; they agree within analytical errors. Therefore, whenever possible, we average all measurements analyzed using both double spike solutions for each sample (Table S1). The data in Fig. 1 were used to estimate the external reproducibility of a *single* measurement (as ±0.12), and typically we need 5–8 repeat measurements to obtain a $2\sigma_m$ uncertainty of <0.06.

3. REPORTING OF CA ISOTOPIC COMPOSITION

It has been agreed in the Ca isotopic community that stable Ca isotopic compositions be reported relative to NIST SRM915a (Hippler et al., 2003; Eisenhauer et al., 2004). This is what we adopted in this study. This high purity Ca reference sample has been proven not to have measurable radiogenic ^{40}Ca excess compared to the Earth's mantle (e.g., Amini et al., 2009; Caro et al., 2010; Huang et al., 2010). In contrast, DePaolo (2004) and Simon and DePaolo (2010) advocated that the stable Ca isotopic compositions be reported relative to the bulk silicate Earth (BSE). Because of the measurable Ca isotopic ($\delta^{44/40}Ca_{SRM915a}$) variations in mantle xenoliths and basalts (e.g., DePaolo, 2004; Amini et al., 2009; Huang et al., 2010; this study), we note that the stable Ca isotopic composition of BSE is a scientific question, and it cannot be directly measured by a single representative sample. In case one needs to convert the values relative to NIST SRM915a to values relative to an arbitrary BSE value, we provide the following conversion equation.

In most cases, the $^{44}Ca/^{40}Ca$ ratio is reported relative to NIST SRM915a (Eq. (1)). If it is reported relative to BSE, we have:

$$\delta^{44/40}Ca^{sample}_{BSE} = \left[\frac{\left(\frac{^{44}Ca}{^{40}Ca}\right)_{sample}}{\left(\frac{^{44}Ca}{^{40}Ca}\right)_{BSE}} - 1\right] \cdot 10^3 \quad (4)$$

The conversion from one to the other can easily be calculated:

$$\delta^{44/40}Ca^{sample}_{BSE} = \frac{\delta^{44/40}Ca^{sample}_{SRM915a} - \delta^{44/40}Ca^{BSE}_{SRM915a}}{\left[1 + 0.001 \cdot \delta^{44/40}Ca^{BSE}_{SRM915a}\right]} \quad (5)$$

Since $\delta^{44/40}Ca^{BSE}_{SRM915a}$ is near 1 (e.g., DePaolo, 2004; Amini et al., 2009; Huang et al., 2010; Simon and DePaolo, 2010), this can be approximated as:

$$\delta^{44/40}Ca^{sample}_{BSE} = \delta^{44/40}Ca^{sample}_{SRM915a} - \delta^{44/40}Ca^{BSE}_{SRM915a} \quad (6)$$

where our current best estimate of $\delta^{44/40}Ca^{BSE}_{SRM915a}$ is 1.05 ± 0.04 (Huang et al., 2010). The error introduced by this approximation is on the order of 1 ppm, much smaller than the typical analytical error.

4. RESULTS

The stable Ca isotopic compositions ($\delta^{44/40}Ca_{SRM915a}$, $\delta^{42/40}Ca_{SRM915a}$ and $\delta^{44/42}Ca_{SRM915a}$) of studied Hawaiian tholeiites are in Table 2. Within analytical errors, all 11 analyzed Hawaiian tholeiites plot along the exponential fractionation trends in the three Ca-isotope plots ($\delta^{44/40}Ca_{SRM915a}$ vs. $\delta^{42/40}Ca_{SRM915a}$ and $\delta^{44/42}Ca_{SRM915a}$) (Fig. 2), implying no measurable radiogenic ^{40}Ca contribution in all measured samples. $\delta^{44/40}Ca_{SRM915a}$ in these Hawaiian tholeiites ranges from 0.75 to 1.02 (Table 2). The highest $\delta^{44/40}Ca_{SRM915a}$ (1.02 ± 0.04) in Hawaiian lavas, found in Mahukona lava 72-1, is similar to that of typical upper mantle (1.05 ± 0.04) (DePaolo, 2004; Amini et al., 2009; Huang et al., 2010; Simon and DePaolo, 2010). The Makapuu-stage Kooolau lavas have the lowest $\delta^{44/40}Ca_{SRM915a}$ (0.75–0.77) within Hawaiian tholeiites (Table 2). The highest and lowest $\delta^{44/40}Ca_{SRM915a}$ (1.02 ± 0.04 in 72-1 vs. 0.75 ± 0.03 in KOO-1) in Hawaiian tholeiites are clearly resolvable with our current analytical precision (Table 2; Fig. 2). More importantly, within Hawaiian tholeiites, $\delta^{44/40}Ca_{SRM915a}$ is negatively correlated with Sr/Nb and $^{87}Sr/^{86}Sr$ (Fig. 3). Note that, the observed $\delta^{44/40}Ca_{SRM915a}$ variation in Hawaiian lavas is not an analytical artifact of applying two spike solutions (Table 1). If only the analyses with the new spike solution are used, there is still measurable $\delta^{44/40}Ca_{SRM915a}$ variation among Hawaiian lavas: Makapuu-stage Koolau lava KOO-1 has $\delta^{44/40}Ca_{SRM915a}$ of 0.75 ± 0.03, which is clearly lower than that in BHVO-1 ($\delta^{44/40}Ca_{SRM915a} = 0.92 \pm 0.03$) (Table S1).

5. DISCUSSION

5.1. The origin of low $\delta^{44/40}Ca_{SRM915a}$

What is the origin of the $\delta^{44/40}Ca_{SRM915a}$ variation within the Hawaiian tholeiites? All our analyzed Hawaiian tholeiites have MgO $\geqslant$ 7%, and olivine is the only phenocryst phase in these tholeiites. Consequently, the observed $\delta^{44/40}Ca_{SRM915a}$ variation cannot be a result of crystal fractionation because of the very low CaO content in olivines. Could it be generated during partial melting of the Hawaiian plume? It was observed that Ca isotopes are fractionated between co-existing clinopyroxene and orthopyroxene from San Carlos and Kilbourne Hole peridotites, implying possible Ca isotopic fractionation in igneous processes (Huang et al., 2010). However, these peridotites were equilibrated under sub-solidus temperatures (~1000 °C) (e.g., Galer and O'Nions, 1989; Hamblock et al., 2007), and the Hawaiian tholeiites were generated at temperatures over 1500 °C (e.g., Putirka, 2005). Since stable isotopic fractionation decreases with increasing temperature, and is proportional to $1/T^2$ (c.f., Schauble, 2004), much smaller Ca isotopic fractionation is expected at mantle solidus temperatures under which Hawaiian tholeiites were generated. Importantly, within Hawaiian tholeiites, $\delta^{44/40}Ca_{SRM915a}$ does not correlate with trace element ratios that are

Table 2
Stable Ca isotopic composition in Hawaiian tholeiites.

	$\delta^{44/40}Ca_{SRM915a}$	2σ	$\delta^{42/40}Ca_{SRM915a}$	2σ	$\delta^{44/42}Ca_{SRM915a}$	2σ	CaO (%)	$^{87}Sr/^{86}Sr$	Sr/Nb	Ba/Y	Nb/Y
Koolau											
Makapuu-stage											
KOO-1	0.75	0.03	0.37	0.04	0.38	0.04	9.46	0.70411	51	3.5	0.34
KOO-7	0.76	0.02	0.37	0.03	0.40	0.03	9.90	0.70410	45	3.2	0.35
KOO-10	0.75	0.05	0.40	0.07	0.35	0.05	8.27	0.70417	50	2.9	0.32
KM-1	0.77	0.03	0.42	0.04	0.34	0.04	7.55		58	4.0	0.31
Kalihi-stage											
KSDP-9	0.92	0.06	0.52	0.07	0.40	0.03	9.18	0.703860	39	2.5	0.29
KSDP-71	0.83	0.06	0.48	0.09	0.35	0.06	10.02	0.703771	34	3.2	0.35
Mahukona											
72-1	1.02	0.04	0.53	0.06	0.50	0.04	12.19	0.703671	33	6.5	0.52
D19-9	0.90	0.05	0.49	0.08	0.41	0.03	6.50	0.703764	30	1.6	0.35
Mauna Kea											
SR685	0.92	0.08	0.49	0.02	0.42	0.07	10.74		23	8.1	0.91
SR700	0.94	0.05	0.49	0.07	0.44	0.06	12.24		22	6.7	0.82
Kilauea											
BHVO-1	0.96	0.05	0.53	0.04	0.44	0.03	11.35	0.703475	21	4.8	0.69

$\delta^{4i/4j}Ca_{SRM915a} = [(^{4i}Ca/^{4j}Ca)_{sample}/(^{4i}Ca/^{4j}Ca)_{SRM915a} - 1] \times 1000$.
We note that, as a tradition, the reported $\delta^{44/40}Ca_{SRM915a}$ in many publications are followed by a "‰" symbol. However, this per mil symbol is redundant following the δ notation definition, and it is very misleading to readers who are not familiar with Ca isotopic studies.
Analytical uncertainty is estimated using the 2 standard error of multiple measurements of each sample (see Table S1).
Element abundances and $^{87}Sr/^{86}Sr$ are from Frey et al. (1994), Roden et al. (1994), Lassiter and Hauri (1998) and Huang et al. (2009).

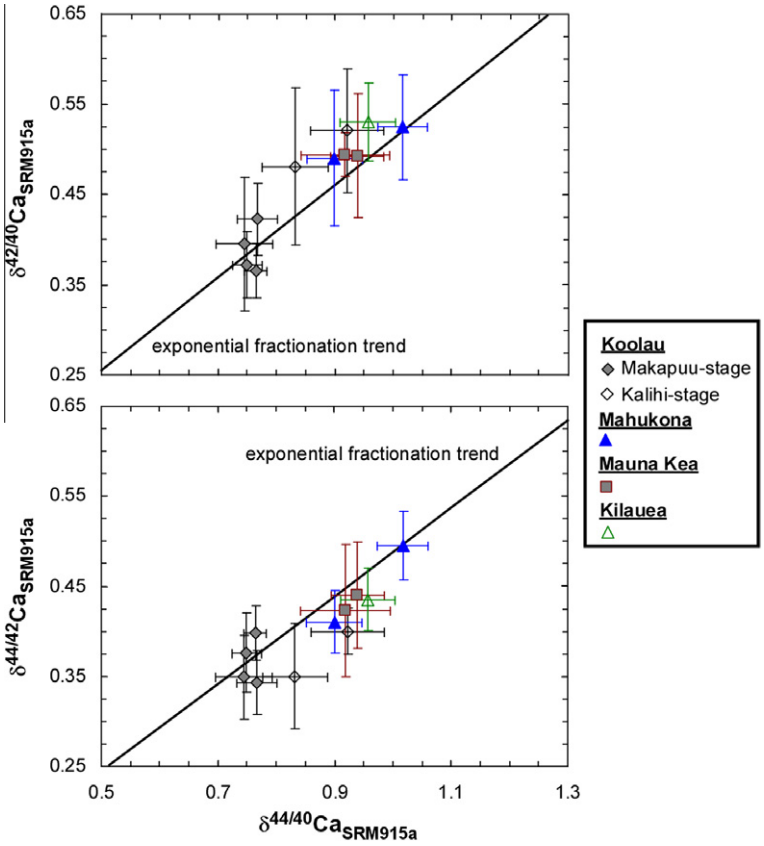

Fig. 2. $\delta^{44/40}Ca_{SRM915a}$ vs. $\delta^{42/40}Ca_{SRM915a}$ and $\delta^{44/42}Ca_{SRM915a}$ in Hawaiian tholeiites. Within analytical errors, all measured samples fall on the exponential fractionation trends.

strongly dependent on the degrees of partial melting, such as Ba/Y and Nb/Y (Fig. 4). Therefore, it is unlikely that the observed $\delta^{44/40}Ca_{SRM915a}$ variation in Hawaiian tholeiites was generated by variable degrees of partial melting of the Hawaiian plume.

With considerable variations, modern marine carbonates (i.e., calcareous limestones), in general, have $\delta^{44/40}Ca_{SRM915a}$ similar to typical mantle values. In contrast, ancient marine carbonates (limestones and dolostones) generally exhibit much lower $\delta^{44/40}Ca_{SRM915a}$ values (usually < 0.5) (e.g., De La Rocha and DePaolo, 2000; Fantle and DePaolo, 2005; Kasemann et al., 2005; Farkaš et al., 2007a,b; Holmden, 2009; Silva-Tamayo et al., 2010). A possible explanation why the global ocean, and thus marine carbonates, gradually evolved through time towards higher $\delta^{44/40}Ca_{SRM915a}$ values (Farkaš et al., 2007b) is that marine carbonates, which preferentially take up light Ca isotopes from seawater (Gussone et al., 2005; Griffith et al., 2008), are being continuously subducted into the Earth's mantle (e.g., Plank and Langmuir, 1993; Dasgupta et al., 2004; DePaolo, 2004). Could this low $\delta^{44/40}Ca_{SRM915a}$ signature in Makapuu-stage Koolau lavas result from assimilation of in situ modern marine carbonates which have low $\delta^{44/40}Ca_{SRM915a}$ similar to those reported by Fantle and DePaolo (2005)? Typical Hawaiian lavas have ~10% CaO. In order to decrease a mantle-like $\delta^{44/40}Ca_{SRM915a}$ of 1.05 to a value (0.75) similar to that observed in Makapuu-stage Koolau lavas, it requires assimilation of 9% carbonate with $\delta^{44/40}Ca_{SRM915a}$ of 0.2. Assimilation of this amount of carbonate leads to an increase of CaO content from 10% to 14%, which is much higher than that in any Hawaiian tholeiites (e.g., Frey et al., 1994; Rhodes and Vollinger, 2004; Table 2).

$\delta^{44/40}Ca_{SRM915a}$ is significantly correlated with Sr/Nb and $^{87}Sr/^{86}Sr$ within Hawaiian tholeiites (Fig. 3). Evidently, the large Sr/Nb (21–58) and, especially, $^{87}Sr/^{86}Sr$ (0.70348–0.70417) variations within Hawaiian tholeiites reflect source heterogeneity (Frey et al., 1994; Roden et al., 1994; Lassiter and Hauri, 1998). Thus, it is most likely that the observed $\delta^{44/40}Ca_{SRM915a}$ variation reflects source heterogeneity. A source component, characterized by high-Sr/Nb (>60) and $-^{87}Sr/^{86}Sr$ (>0.704), and low-$\delta^{44/40}Ca_{SRM915a}$ (<0.65), is inferred, and it is best manifested in Makapuu-stage Koolau lavas.

This low-$\delta^{44/40}Ca_{SRM915a}$ source component fits best with recycled ancient marine carbonates. As discussed above, ancient marine carbonates have low $\delta^{44/40}Ca_{SRM915a}$ (e.g., Kasemann et al., 2005; Farkaš et al., 2007a,b; Holmden, 2009; Silva-Tamayo et al., 2010).

Marine carbonates are also characterized by high Sr/Nb (e.g., Plank and Langmuir, 1998), because Sr can replace Ca in the carbonate mineral structures. Although ancient carbonates have low Rb/Sr, they are still characterized by radiogenic $^{87}Sr/^{86}Sr$. The seawater $^{87}Sr/^{86}Sr$ was already very radiogenic (>0.704) at 2 Ga (Shields and Veizer, 2002), owing to the radiogenic $^{87}Sr/^{86}Sr$ input from riverine

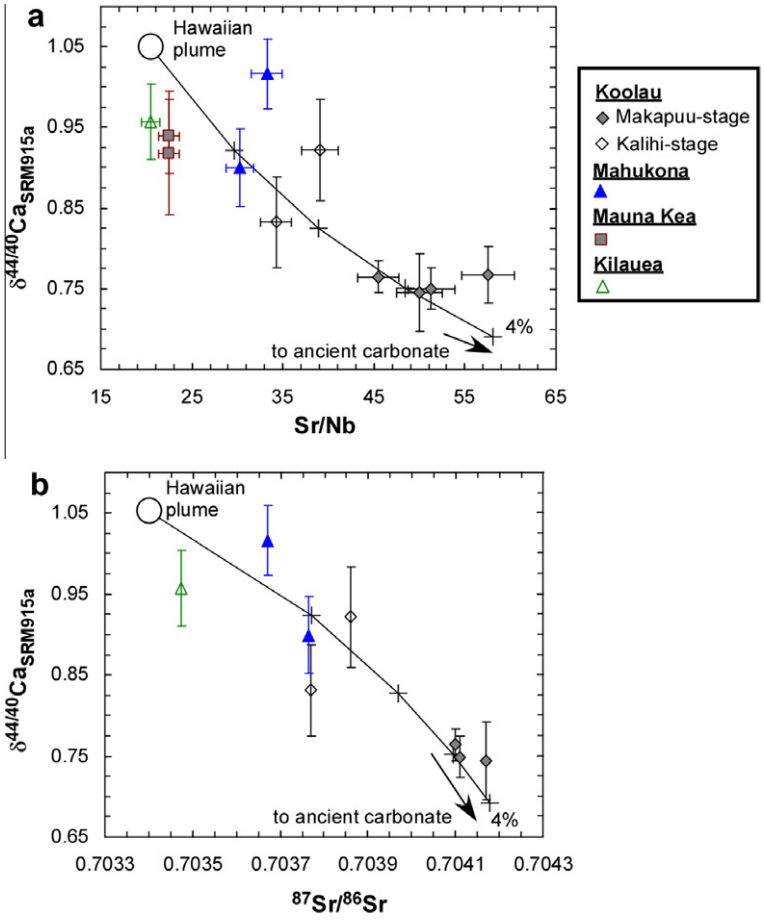

Fig. 3. $\delta^{44/40}Ca_{SRM915a}$ vs. Sr/Nb and $^{87}Sr/^{86}Sr$ in Hawaiian tholeiites. The relative error bar on Sr/Nb is taken as 5%, reflecting typical analytical uncertainty of the solution ICP–MS measurements. The error bar on $^{87}Sr/^{86}Sr$ is smaller than the symbol. The $\delta^{44/40}Ca_{SRM915a}$ vs. Sr/Nb trend has $R^2 = 0.67$, and the $\delta^{44/40}Ca_{SRM915a}$ vs. $^{87}Sr/^{86}Sr$ trend has $R^2 = 0.77$, suggesting that both correlations are significant and meaningful. These two trends can be reproduced by adding a recycled ancient carbonate component ([CaO] = 56%, [Sr] = 800 ppm, [Nb] = 0, $\delta^{44/40}Ca_{SRM915a} = 0.2$ and $^{87}Sr/^{86}Sr = 0.7046$) to a plume component. The plume component is assumed to have primitive mantle-like CaO and Sr contents (3.21% and 18.21 ppm, respectively) (Hofmann, 1988) and $\delta^{44/40}Ca_{SRM915a}$ (1.05) (DePaolo, 2004; Amini et al., 2009; Huang et al., 2010), Sr/Nb = 20.53, and $^{87}Sr/^{86}Sr = 0.7034$ (Table 3). The maximum amount of carbonate added (4%) is labeled at the end of the model mixing lines, and the tick marks represent 1% increments.

weathering of the upper continental crust. Our model calculation shows that the negative $\delta^{44/40}Ca_{SRM915a}$ vs. Sr/Nb and $^{87}Sr/^{86}Sr$ trends of Hawaiian tholeiites can be explained by adding up to 4% recycled ancient marine carbonates (with $\delta^{44/40}Ca_{SRM915a} = 0.2$) to a plume component with typical mantle $\delta^{44/40}Ca_{SRM915a}$ value of 1.05, with the largest amount (4%) of recycled ancient marine carbonates in the source of Makapuu-stage Koolau lavas (Fig. 3; Table 3). With this interpretation, a mass-balance calculation (Table 3) shows that 40% of the Ca budget and 65% of the Sr budget of Makapuu-stage Koolau lavas come from the recycled ancient marine carbonates. The Hawaiian volcanism has been active for over 80 Myrs (Duncan and Keller, 2004), if the recycled ancient carbonate component, best sampled by Makapuu-stage Koolau lavas, is common in all Hawaiian–Emperor volcanoes, it will significantly affect our understanding of the global Ca and Sr cycles.

Although Hawaiian lavas show an overall negative $^{87}Sr/^{86}Sr$–$^{143}Nd/^{144}Nd$ trend, in detail, lavas from Koolau, Lanai and Kahoolawe show sub-parallel trends with considerable $^{87}Sr/^{86}Sr$ variation at a given $^{143}Nd/^{144}Nd$ (e.g., Fig. 5 of Huang et al., 2005; Fig. 3 of Tanaka et al., 2008). In contrast, $^{143}Nd/^{144}Nd$ is highly correlated with $^{176}Hf/^{177}Hf$ at Hawaii (e.g., Blichert-Toft et al., 1999; Huang et al., 2005; Tanaka et al., 2008). The decoupling of $^{87}Sr/^{86}Sr$ from $^{143}Nd/^{144}Nd$ and $^{176}Hf/^{177}Hf$ implies a source component with very high Sr/Nd and Sr/Hf ratios (Huang et al., 2005). At Hawaii, two types of high-Sr/Nd and -Sr/Hf components have been proposed: recycled ancient carbonate-rich sediment (Huang and Frey, 2005; this study) and recycled ancient gabbroic crust (Sobolev et al., 2000; Huang et al., 2005). These two components have different $^{87}Sr/^{86}Sr$ signatures: recycled ancient carbonates have very radiogenic $^{87}Sr/^{86}Sr$, and recycled ancient gabbros have very low $^{87}Sr/^{86}Sr$ because of low Rb/Sr ratio. Variable amounts of these two components could explain the two sub-parallel $^{87}Sr/^{86}Sr$–$^{143}Nd/^{144}Nd$ trends of Koolau and Kahoolawe (Fig. 5 of Huang et al., 2005). Currently, there is no Ca isotopic data on gabbroic crusts, which are plagioclase cumulates. Such data can provide

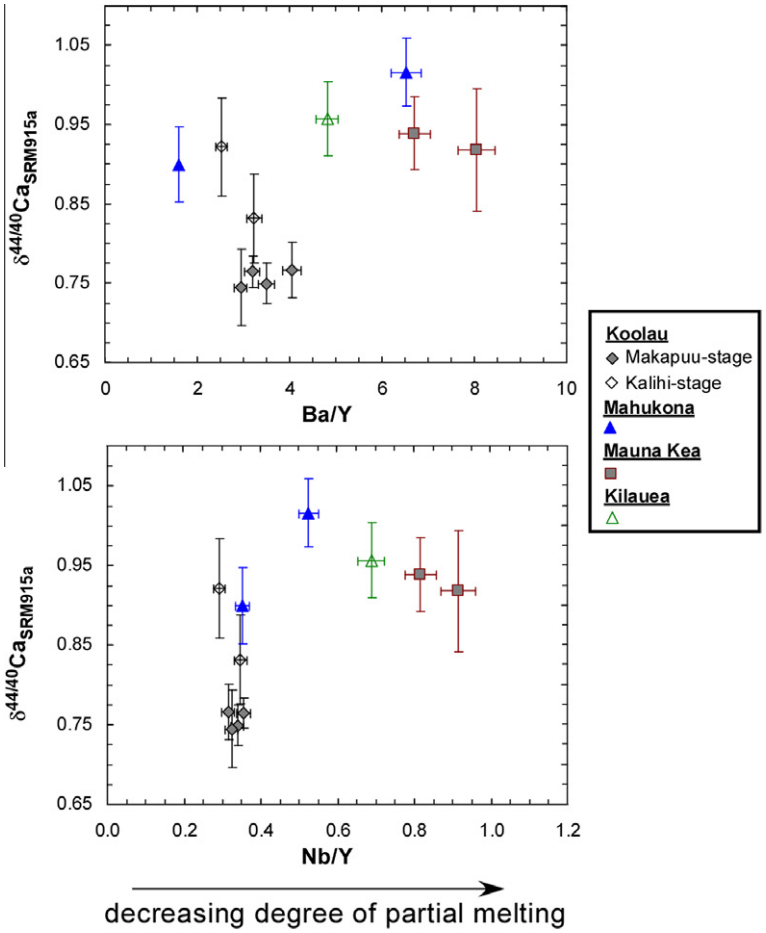

Fig. 4. $\delta^{44/40}Ca_{SRM915a}$ vs. Ba/Y and Nb/Y in Hawaiian tholeiites. The relative error bars on Ba/Y and Nb/Y are taken as 5%, reflecting typical analytical uncertainty of the solution ICP-MS measurements. The lack of correlation between $\delta^{44/40}Ca_{SRM915a}$ and Ba/Y and Nb/Y, trace element abundance ratios that are sensitive to partial melting, suggests that the observed $\delta^{44/40}Ca_{SRM915a}$ variation in Hawaiian tholeiites is not caused by partial melting of the Hawaiian plume.

Table 3
Input and output model parameters for Fig. 3.

	[CaO] (%)	[Sr] (ppm)	[Nb] (ppm)	Sr/Nb	$\delta^{44/40}Ca_{SRM915a}$	$^{87}Sr/^{86}Sr$		
Hawaiian plume	3.21	18.21	0.89	20.5	1.05	0.70340		
Ancient carbonate	56	800	0		0.20	0.70460		
carbonate added in the mixtures (%)							Ca budget from carbonate (%)	Sr budget from carbonate (%)
0	3.21	18.21	0.89	20.5	1.05	0.70340	0	0
1	3.74	26.03	0.88	29.6	0.92	0.70377	15	31
2	4.27	33.85	0.87	38.9	0.83	0.70397	26	47
3	4.79	41.66	0.86	48.4	0.75	0.70409	35	58
4	5.32	49.48	0.85	58.1	0.69	0.70418	42	65

further constraints on testing the idea that recycled ancient gabbros are present in the Hawaiian plume (Sobolev et al., 2000; Huang et al., 2005).

5.2. The effect of recycled, ancient carbonate-rich sediment on CaO contents

Recycled ancient marine sediments are thought to be important in the petrogenesis of Hawaiian lavas (Frey et al., 1994; Lassiter and Hauri, 1998; Blichert-Toft et al., 1999). Further detailed studies show that this ancient sedimentary component is carbonate-rich (Huang and Frey, 2005; Huang et al., 2009; this study). How was this recycled, ancient carbonate-rich sedimentary component sampled? In Section 4.1 (Fig. 3), we adopted the following model: The recycled, ancient carbonate was mixed into a peridotite to form an enriched peridotite, which then partial melted to form Hawaiian tholeiites. We modeled its effect on

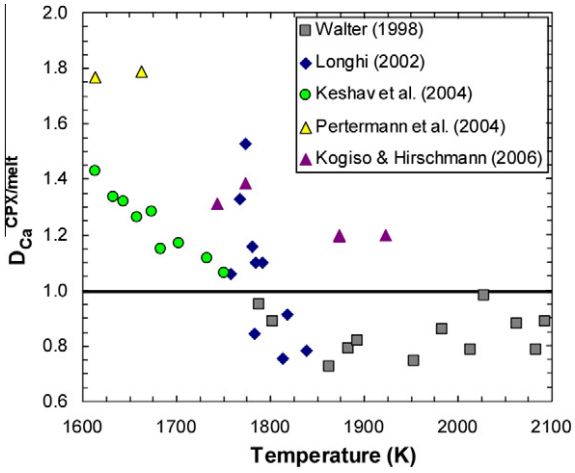

Fig. 5. Temperature dependence of $D_{Ca}^{clinopyroxene/melt}$. The temperature–$D_{Ca}^{clinopyroxene/melt}$ correlation is better shown using experiments from single study, for example, Keshav et al. (2004). At a given temperature, there is considerable $D_{Ca}^{clinopyroxene/melt}$ variation, ranging from incompatible (<1) to compatible (>1).

$\delta^{44/40}$Ca but what is its effect on major element compositions? We are particularly interested in the CaO content.

We model this effect using available partial melting experiments (e.g., Walter, 1998; Longhi, 2002; Keshav et al., 2004; Pertermann et al., 2004; Kogiso and Hirschmann, 2006). During partial melting of garnet peridotite, clinopyroxene is the major host of Ca (e.g., Walter, 1998; Longhi, 2002), thus the behavior of Ca is mainly controlled by the Ca partition coefficient between clinopyroxene and melt, $D_{Ca}^{CPX/melt}$. As shown in Fig. 5, $D_{Ca}^{CPX/melt}$ varies from 0.7 to 1.8, and shows a strong negative correlation with temperature. This is consistent with the more commonly known fact that clinopyroxene becomes more similar to orthopyroxene at higher temperature. At a given temperature, there is considerable $D_{Ca}^{CPX/melt}$ variation. Further, the melting reaction of garnet peridotite is variable. For example, the melting reactions proposed by Salters (1996) and Longhi (2002) consume more clinopyroxene than that by Walter (1998). In order to show the effects of the above discussed uncertainties, we consider two cases here (Table 4). In Case I, we use the melting reaction and the average Ca partition coefficients from Walter (1998). In Case II, we use the melting reaction from Salters (1996). We keep $D_{Ca}^{OPX/melt}$ and $D_{Ca}^{GRT/melt}$ the same as those in Case I, but change $D_{Ca}^{CPX/melt}$ to 1.20 (Fig. 5). In both cases, the starting peridotite is composed of 53% olivine, 18% orthopyroxene, 27% clinopyroxene and 2% garnet (Table 4; Table 8 of Walter, 1998). We use a non-modal batch melting model:

$$C_l/C_o = 1/[D + F(1 - P)] \quad (7)$$

where C_l and C_o are the element abundances in the partial melt and the original source; F is the degree of partial melting; D is the bulk solid-melt partition coefficient; and P is the bulk solid-melt partition coefficient for the melting assemblage of minerals.

The model results are in Fig. 6. In Case I, the CaO content in the melt decreases with increasing degree of partial melting. This mimics the Ca behavior shown in Fig. 5 of Walter (1998). In contrast, in Case II, the CaO content in the melt increases with increasing degree of partial melting, similar to the experimental result of Kushiro (1996), see his Fig. 6, and the model result shown in Fig. 13d of Stolper et al. (2004) who used the algorithm from Longhi (2002).

Table 4
Input model parameters for Fig. 6.

	Peridotite[a]	Peridotite plus 2% $CaCO_3$[b]
SiO_2	44.90	44.77
TiO_2	0.16	0.16
Cr_2O_3	0.41	0.41
Al_2O_3	4.26	4.25
FeO	8.02	8.00
MgO	37.30	37.19
CaO	3.45	4.55
MnO	0.13	0.13
NiO	0.24	0.24
Na_2O	0.22	0.22
K_2O	0.09	0.09

	Peridotite[a]	Peridotite plus 2% $CaCO_3$[b]	Case I[a]		Case II[c]	
			Melting reaction coefficient	$D_{Ca}^{mineral/melt}$	Melting reaction coefficient	$D_{Ca}^{mineral/melt}$
Olivine	0.53	0.56	0.08	0	0.05	0
Orthopyroxene	0.18	0.01	−0.19	0.24	−0.49	0.24
Clinopyroxene	0.27	0.40	0.81	0.84	1.31	1.20
Garnet	0.02	0.03	0.30	0.46	0.13	0.46

[a] The peridotite composition, phase proportions, melting reaction and partition coefficients are from Walter (1998).
[b] 2% $CaCO_3$ is added into the original peridotite, then major element compositions are re-normalized to 100%. Major element compositions are re-distributed among the four phases, whose compositions are from Run 30.05 of Walter (1998).
[c] Melting reaction is from Salters (1996). The clinopyroxene-melt partition coefficient of Ca is taken as 1.20. See text for details.

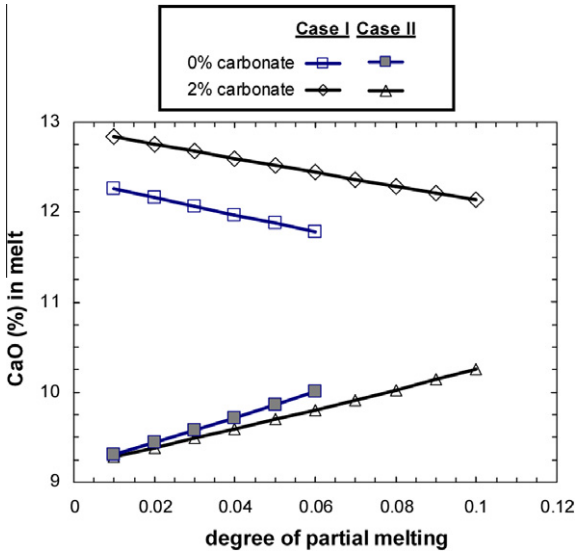

Fig. 6. Model results of CaO content in partial melts as a function of degree of partial melting. The model input parameters are in Table 4. Non-modal batch melting is used in all cases.

This type of behavior is caused by the high $D_{Ca}^{CPX/melt}$ (1.20) and the large melting reaction coefficient for clinopyroxene (1.31), which lead to a P value of 1.5 for Ca.

We further model the effect of carbonate by adding 2% carbonate into the starting peridotite. Assuming that carbonate is broken down and CO_2 is released, adding 2% carbonate into the starting peridotite results in an enriched peridotite with 56% olivine, 1% orthopyroxene, 40% clinopyroxene and 3% garnet (Table 4). The phase proportions are calculated by re-distributing all major elements into the four phases, using the mineral compositions of Run 30.05 from Walter (1998). The net effect is to increase the clinopyroxene proportion at the expense of orthopyroxene (Table 4). Fig. 6 shows the model results using a non-modal batch melting model. In Case I, adding carbonate into a peridotite results in higher CaO content in the melts. This is a consequence of the incompatible behavior of Ca during partial melting of garnet peridotite (Table 4; Walter, 1998). In contrast, in Case II, the effect of adding carbonate is to slightly lower the CaO content in the melts. This is because increasing CaO content in the source leads to a higher proportion of clinopyroxene, and Ca is compatible in clinopyroxene in Case II.

In summary, the uncertainties of $D_{Ca}^{CPX/melt}$ and the melting reaction in the published studies make it hard to precisely predict the CaO abundance effect of adding carbonante into a peridotite. The low CaO content of Makapuu-stage Koolau lavas (Frey et al., 1994) has been interpreted as a result of sampling a dacite or basaltic andersite component (Pertermann et al., 2004; Huang and Frey, 2005; Sobolev et al., 2005, 2007; Huang et al., 2007). Herzberg (2006) further argued that most Hawaiian tholeiites have CaO too low to be partial melts of garnet peridotite. However, given the large variation of $D_{Ca}^{CPX/melt}$ (Fig. 5) in the published studies and the fact that clinopyroxene is the largest Ca host in the mantle, these results need to be re-evaluated.

6. SUMMARY

We observed a systematic stable Ca isotopic variation in Hawaiian tholeiites. $\delta^{44/40}Ca_{SRM915a}$ in Hawaiian tholeiites ranges from 0.75 to 1.02, and it covers over 20% of the $\delta^{44/40}Ca_{SRM915a}$ variations found in global modern and ancient carbonates. More importantly, the stable Ca isotopic ratios are correlated with Sr/Nb and $^{87}Sr/^{86}Sr$, which are all geochemical parameters controlled by recycled ancient marine carbonates. Specifically, within Hawaiian tholeiites, Makapuu-stage Koolau lavas sampled the largest amount (up to 4%) of this recycled ancient marine carbonate component. Because of the uncertainties in Ca partition coefficient between clinopyroxene and melt in the published studies, the effect of adding carbonate into mantle peridotite on CaO content in the melts, however, cannot be precisely modeled at this stage.

The large stable Ca isotopic variation observed in Hawaiian tholeiites leads to the following questions: Is the stable Ca isotopic variation a special feature of Hawaiian lavas? How variable are the Ca isotopic compositions in MORBs and OIBs? What percentages of Ca and Sr budgets in the mantle are from recycled material? And what constraints do they provide on the understanding of global Ca, C and Sr cycles, and their roles in the chemical evolution of seawater and the Earth's climate through geological timescale? These can only be answered with further detailed Ca isotopic studies of the global Ca cycle and its various components, including MORBs and OIBs.

ACKNOWLEDGEMENTS

This work was supported by NSF award EAR-0951487. We thank J.I. Simon and an anonymous reviewer for their constructive comments, and A.D. Brandon for his excellent editorial handling.

APPENDIX A. SUPPLEMENTARY DATA

Supplementary data associated with this article can be found, in the online version, at doi:10.1016/j.gca.2011.06.010.

REFERENCES

Amini M., Eisenhauer A., Böhm F., Holmden C., Kreissig K., Hauff F. and Jochum K. P. (2009) Calcium Isotopes ($\delta^{44/40}Ca$) in MPI-DING reference glasses, USGS rock powders and various rocks: evidence for Ca isotope fractionation in terrestrial silicates. *Geostand. Newsl.* **33**, 231–247.

Blichert-Toft J., Frey F. A. and Albarède F. (1999) Hf isotope evidence for pelagic sediments in the source of Hawaiian basalts. *Science* **285**, 879–882.

Brandon A. D., Norman M. D. and Walker R. J. (1999) J. W. Morgan, ^{186}Os–^{187}Os systematics of Hawaiian picrites. *Earth Planet. Sci. Lett.* **172**, 25–42.

Caro G., Papanastassiou D. A. and Wasserburg G. J. (2010) ^{40}K–^{40}Ca isotopic constraints on the oceanic calcium cycles. *Earth Planet. Sci. Lett.* **296**, 124–132.

Dasgupta R., Hirschmann M. M. and Withers A. C. (2004) Deep global cycling of carbon constrained by the solidus of anhydrous, carbonated eclogite under upper mantle conditions.

Earth Planet. Sci. Lett. **227**, 73–85. doi:10.1016/j.epsl.2004.08.004.

De La Rocha C. and DePaolo D. J. (2000) Isotopic evidence for variations in the marine calcium cycle over the Cenozoic. *Science* **289**, 1176–1178. doi:10.1126/science.289.5482.1176.

DePaolo D. J. (2004). Calcium isotopic variations produced by biological, kinetic, radiogenic and nucleosynthetic processes. Chapter in *Reviews in Mineralogy and Geochemistry* (ed. Jodi Rosso), **55**, pp. 255–288.

Duncan R. A. and Keller R. A. (2004). Radiometric ages for basement rocks from the Emperor seamounts, ODP Leg 197. *Geochem. Geophys. Geosys.* 5, Q08L03, doi:10.1029/2004GC000704.

Eiler J. M., Farley K. A., Valley J. W., Hofmann A. and Stolper E. M. (1996) Oxygen isotope constraints on the sources of Hawaiian volcanism. *Earth Planet. Sci. Lett.* **144**, 453–468.

Eisenhauer A., Nagler T., Stille P., Kramers J., Gussone N., Bock B., Fietzke J., Hippler D. and Schmitt A.-D. (2004) Proposal for an international agreement on Ca notation as a result of the discussion from the workshop on stable isotope measurements in Davos (Goldschmidt 2002) and Nice (EGS-AGU-EUG 2003). *Geostand. Geoanal. Res.* **28**, 149–151.

Fantle M. S. and DePaolo D. J. (2005) Variations in the marince Ca cycle over the past 20 million years. *Earth Planet. Sci. Lett.* **237**, 102–117.

Farkaš J., Buhl D., Blenkinsop J. and Veizer J. (2007a) Evolution of the oceanic calcium cycle during the late Mesozoic: evidence from $\delta^{44/40}$Ca of marine skeletal carbonates. *Earth Planet. Sci. Lett.* **253**, 96–111.

Farkaš J., Bohm F., Wallmann K., Blenkinsop J., Eisenhauer A., Geldren R. V., Munnecke A., Voigt S. and Veizer J. (2007b) Calcium isotope record of phanerozoic oceans: implications for chemical evolution of seawater and its causative mechanisms. *Geochim. Cosmochim. Acta* **71**, 5117–5134.

Frey F. A., Garcia M. O. and Roden M. F. (1994) Geochemical characteristics of Koolau Volcano: implications of intershield geochemical differences among Hawaiian volcanoes. *Geochim. Cosmochim. Acta* **58**, 1441–1462.

Galer S. J. G. and O'Nions R. K. (1989) Chemical and isotopic studies of ultramafic inclusions from the San Carlos volcanic field, Arizona: a bearing on their petrogenesis. *J. Petrol.* **30**, 1033–1064.

Griffith E. M., Paytan A., Caldeira K., Bullen T. D. and Thomas E. (2008) A dynamic marine Ca cycle during the past 28 million years. *Science* **322**, 1671–1674.

Gussone N., Böhm F., Eisenhauer A., Dietzel M., Heuser A., Teichert B. M. A., Reitner J., Wörheide G. and Dullo W.-C. (2005) Calcium isotope fractionation in calcite and aragonite. *Geochim. Cosmochim. Acta* **69**, 4485–4494.

Hamblock J. M., Andronicos C. L., Miller K. C., Barnes C. G., Ren M.-H., Averill M. G. and Anthony E. Y. (2007) A composite geologic and seismic profile beneath the southern Rio Grande rift, New Mexico, based on xenolith mineralogy, temperature, and pressure. *Tectonophysics* **442**, 14–48.

Herzberg C. (2006) Petrology and thermal structure of the Hawaiian plume from Mauna Kea volcano. *Nature* **444**, 605–609. doi:10.1038/nature05254.

Heuser A., Eisenhauer A., Boehm F., Wallmann K., Gussone N., Pearson P. N., Naegler T. F. and Dullo W.-Ch. (2005) Calcium isotope ($\delta^{44/40}$Ca) variations of Neogene planktonic foraminifera. *Paleoceanography* 20, PA2013. doi:10.1029/2004PA001048.

Heuser A., Eisenhauer A., Gussone N., Bock B., Hansen B. T. and Nägler T. F. (2002) Measurement of calcium isotopes ($\delta^{44/40}$Ca) using a multicollector TIMS technique. *Int. J. Mass Spectrom.* **220**, 387–399.

Hippler D., Schmitt A.-D., Gussone N., Heuser A., Stille P., Eisenhauer A. and Nägler T. F. (2003) Calcium isotopic composition of various reference materials and seawater. *Geostand. Newsl.* **27**, 13–19.

Hofmann A. W. (1988) Chemical differentiation of the Earth: the relationship between mantle, continental crust, and oceanic crust. *Earth Planet. Sci. Lett.* **90**, 297–314.

Holmden Ch. (2009) Ca isotope study of ordovician dolomite, limestone, and anhydrite in the Williston basin: implications for subsurface dolomitisation and local Ca cycling. *Chem. Geol.* **268**, 180–188.

Huang S. and Frey F. A. (2005) Recycled oceanic crust in the Hawaiian plume: evidence from temporal geochemical variations within the Koolau shield. *Contrib. Mineral. Petrol.* **149**, 556–575. doi:10.1007/s00410-005-0664-9.

Huang S., Frey F. A., Blichert-Toft J., Fodor R. V., Bauer G. R. and Xu G. (2005) Enriched components in the Hawaiian plume: evidence from Kahoolawe volcano, Hawaii. *Geochem. Geophys. Geosyst.* **6**, Q11006. doi:10.1029/2005GC001012.

Huang S., Humayun M. and Frey F. A. (2007) Iron/Manganese ratio and manganese content in shield lavas from Koolau Volcano, Hawaii. *Geochim. Cosmochim. Acta.* **71**, 4557–4569. doi:10.1016/j.gca.2007.07.013.

Huang S., Abouchami W., Blichert-Toft J., Clague D. A., Cousens B. L., Frey F. A. and Humayun M. (2009) Ancient carbonate sedimentary signature in the Hawaiian plume: evidence from Mahukona volcano, Hawaii. *Geochem. Geophys. Geosyst.* **10**, Q08002. doi:10.1029/2009GC002418.

Huang S., Farkaš J. and Jacobsen, S. B. (2010) Calcium isotopic fractionation between clinopyroxene and orthopyroxene from Mantle peridotites. *Earth Planet. Sci. Lett.* **292**, 337–344. doi:10.1016/j.epsl.2010.01.042.

Humayun M., Qin L. and Norman M. D. (2004) Geochemical evidence for excess iron in the mantle beneath Hawai'i. *Science* **306**, 91–94.

Kasemann S. A., Hawkesworth Ch. J., Pravec A. R., Fallick P. N. and Pearson P. N. (2005) Boron and calcium isotope composition in Neoproterozoic carbonate rocks from Namibia: evidence for extreme environmental change. *Earth Planet. Sci. Lett.* **231**, 73–86.

Keshav S., Gudfinnsson G. H., Sen G. and Fei Y. (2004) High-pressure melting experiments on garnet clinopyroxenite and the alkalic to tholeiitic transition in ocean-island basalts. *Earth Planet. Sci. Lett.* **223**, 365–379.

Kogiso T. and Hirschmann M. M. (2006) Partial melting experiments of bimineralic eclogite and the role of recycled oceanic crust in the genesis of ocean island basalts. *Earth Planet. Sci. Lett.* **249**, 188–199.

Kushiro I. (1996) Partial melting of a fertile mantle peridotite at high pressures: an experimental study using aggregates of diamond Monogr. *Am. Geophys. Union* **95**, 109–122.

Lassiter J. C. and Hauri E. H. (1998) Osmium-isotope variations in Hawaiian lavas: evidence for recycled oceanic lithosphere in the Hawaiian plume. *Earth Planet. Sci. Lett.* **164**, 483–496.

Longhi J. (2002) Some phase equilibrium systematics of lherzolite melting: I. *Geochem. Geophys. Geosyst.* **3**(3). doi:10.1029/2001GC000204.

Montelli R., Nolet G., Dahlen F. A., Masters G., Engdahl E. R. and Hung S.-H. (2004) Finite-frequency tomography reveals a variety of plumes in the mantle. *Science* **303**, 338–343.

Pertermann M., Hirschmann M. M., Hametner K., Gunther D. and Schmidt M. W. (2004) Experimental determination of trace element partitioning between garnet and silica-rich liquid during anhydrous partial melting of MORB-like eclogite. *Geochem. Geophys. Geosyst.* **5**, Q05A01. doi:10.1029/2003GC000638.

Plank T. and Langmuir C. (1993) Tracing trace elements from sediment input to volcanic output at subduction zones. *Nature* **362**, 739–742.

Plank T. and Langmuir C. H. (1998) The chemical composition of subducting sediment and its consequences for the crust and mantle. *Chem. Geol.* **145**, 325–394.

Putirka K. D. (2005) Mantle potential temperatures at Hawaii, Iceland, and the mid-ocean ridge system, as inferred from olivine phenocrysts: evidence for thermally driven mantle plumes. *Geochem. Geophys. Geosyst.* **6**, Q05L08. doi:10.1029/2005GC000915.

Rhodes J. M. and Vollinger M. J. (2004) Composition of basaltic lavas sampled by phase-2 of the Hawaii scientific drilling project: geochemical stratigraphy and magma types. *Geochemistry Geophysics. Geosystems* **5**, Q03G13. doi:10.1029/2002GC000434.

Roden M. F., Trull T., Hart S. R. and Frey F. A. (1994) New He, Sr, Nd and Pb isotopic constraints on the constitution of the Hawaiian plume: results from Koolau volcano, Oahu, Hawaii. *Geochim. Cosmochim. Acta.* **58**, 1431–1440.

Russell W. A., Papanastassiou D. A. and Tombrello T. A. (1978) Ca isotope fractionation on the Earth and other solar system materials. *Geochim. Cosmochim. Acta* **42**, 1075–1090.

Salters V. J. M. (1996) The generation of mid-ocean ridge basalts from the Hf and Nd isotope perspective. *Earth Planet. Sci. Lett.* **141**, 109–123.

Schauble E. A. (2004) Applying stable isotope fractionation theory to new systems. In *Geochemistry of Non-traditional Stable Isotopes* (eds. C. M. Johnson, B. Beard and F. Albarède). Rev. Mineral. Geochem. **55**, pp. 65–111.

Shields G. and Veizer J. (2002) Precambrian marine carbonate isotope database: Version 1.1. *Geochem. Geophys. Geosyst.* **3**(6). doi:10.1029/2001GC000266.

Silva-Tamayo J. C., Nagler T. F., Villa I. M., Kyser K., Vieira L. C., Sial A. N., Narbonne G. M. and James N. P. (2010) Global Ca isotope variations in c. 0.7 Ga old post-glacial carbonate successions. *Terra Nova* **22**, 188–194.

Simon J. I. and DePaolo D. J. (2010) Stable calcium isotopic composition of meteorites and rocky planets. *Earth Planet. Sci. Lett.* **289**, 457–466.

Sobolev A. V., Hofmann A. W. and Nikogosian I. K. (2000) Recycled oceanic crust observed in ghost plagioclase within the source of Mauna Loa lavas. *Nature* **404**, 986–990.

Sobolev A. V., Hofmann A. W., Sobolev S. V. and Nikogosian I. K. (2005) An olivine free mantle source of Hawaiian shield basalts. *Nature* **434**, 590–597. doi:10.1038/nature03411.

Sobolev A. V., Hofmann A. W., Kuzmin D. V., Yaxley G. M., Arndt N. T., Chung S.-L., Garcia M. O., Gurenko A. A., Danyushevsky L. V., Elliott T., Frey F. A., Kamenetsky V. S., Kerr A. C., Krivolutskaya N. A., Matvienkov V. V., Nikogosian I. K., Rocholl A., Suschevskaya N. M. and Teklay M. (2007) The amount of recycled crust in sources of mantle-derived melts. *Science* **316**, 412–417. doi:10.1126/science.1138113.

Stolper E., Sherman S., Garcia M. and Baker Seaman C. (2004) Glass in the submarine section of the HSDP2 drill core, Hilo, Hawaii. *Geochem. Geophys. Geosyst.* **5**(7), Q07G15. doi:10.1029/2003GC000553.

Tanaka R., Makishima A. and Nakamura E. (2008) Hawaiian double volcanic chain triggered by an episodic involvement of recycled material: constraints from temporal Sr–Nd–Hf–Pb isotopic trend of the Loa-type volcanoes. *Earth Planet. Sci. Lett.* **265**, 450–465.

Walter M. J. (1998) Melting of garnet peridotite and the origin of Komatiite and depleted lithosphere. *J. Petrol.* **39**(1), 29–60.

Associate editor: Alan D. Brandon